

1 **New *Phytologist* Supporting Information**

2 Article title: A core microbiome in the hyphosphere of arbuscular mycorrhizal fungi has
3 functional significance in organic phosphorus mineralization

4 Authors: Letian Wang^{1§}, Lin Zhang^{1§}, Timothy S. George², Gu Feng^{1*}

5 Article acceptance date: 18 November 2022

6

7 The following Supporting Information is available for this article:

8 **Methods S1** Details of the experimental set-up.

9 **Fig. S1** Details of the experimental sites and experimental system. **a** Geographical
10 location of the three experimental sites in China. **b** The in-growth tubes were buried to
11 a depth of 20-30 cm in soil and 15 cm away from the plants. PVC tubes (12 cm in
12 diameter, 5 cm in length) were sealed with 30 µm mesh (permitting AM fungal hyphae
13 but not roots to grow into) or 0.45 µm membrane (excluding AM fungal hyphae and
14 roots to grow into) in the two ends, respectively. **c** Schematic drawing of the in-growth
15 tubes. **d** Schematic drawing of the two-compartment cultivation system (microcosm)
16 used in the pot experiment. The microcosm is divided into a root compartment and a
17 hyphal compartment by two 30 µm nylon meshes and a buffer zone. **e** The hyphae
18 accumulated on the surface of the membranes. AM fungal hyphae were manually
19 collected using a stereoscope, according to their different characteristics from other
20 fungi. AM fungal hyphae are colorless and transparent, and have no septum. The
21 collected hyphae were washed five times in washing buffers (0.01 M Phosphate buffer
22 saline, pH = 7) to remove the adhered soil.

23 **Fig. S2** The ratio of AM fungal to total fungal DNA copy number in hyphal samples across
24 three sites. The higher the ratio, the greater the proportion of AM fungi in our hyphal samples.
25 Control indicates the pure AM fungal hyphal samples collected from AM fungal inoculum.
26 Values are means (n = 8) and bars represent standard errors.

27 **Fig. S3** Rarefaction curve of OTUs for individual sample across the different datasets:
28 **a** AM fungal 18S rRNA gene dataset in Experiment 1, **b** hyphosphere and bulk soil
29 bacterial 16S rRNA gene dataset in Experiment 1, **c** hyphosphere and bulk soil bacterial
30 16S rRNA gene dataset in Experiment 2.

31 **Fig. S4** Mycorrhizal colonization (**a**) of host plants and hyphal length density (**b**) in the
32 in-growth tubes at each site. Values are means (n = 8) and bars represent standard errors.

33 **Fig. S5** Correlation matrix (Spearman) of phosphatase activities and soil properties in
34 the tubes across the three sites. Positive correlations are displayed in red and negative

35 correlations in blue. Color intensity is proportional to the correlation coefficients.
36 Correlations significant at $P < 0.05$ were not marked with a cross.

37 **Fig. S6** Box plot showing Shannon-Wiener diversity indices (**a**) and observed species
38 indices (**b**) for three communities (AM fungi, hyphosphere and bulk soil bacteria). For
39 each community, the asterisk indicates significant difference among three sites. The
40 asterisk on the solid line represented the significant difference between bacteria in the
41 hyphosphere and bulk soil. Boxes show first quartile, median and third quartile.
42 Whiskers extend to the most extreme points within $1.5 \times$ box length, and the points are
43 values that fall outside the whiskers. * $P < 0.05$, ** $P < 0.01$, *** $P < 0.001$, **** $P <$
44 0.0001 . ns, no significance.

45 **Fig. S7** Bipartite networks display experimental site-sensitive OTUs (*ssOTUs*) in bulk
46 soil (**a**) and hyphosphere (**b**) bacterial communities. Circles represented individual
47 bacterial OTUs that are positively and significantly associated ($P < 0.05$) with one or
48 more of sites (associations given by connecting lines). OTUs were colored according
49 to their phyla assignment. **c** Qualitative taxonomic composition of experimental site-
50 insensitive OTUs (non-*ssOTUs*) is reported as proportional OTUs numbers per class.

51 **Fig. S8** *hsOTUs* are largely conserved at the class levels across three experimental sites.
52 Phylogenetic characterization was conducted using a neighbor-joining model of 82
53 *hsOTUs*. Circles represent non-*ssOTUs* and triangles represent *ssOTUs*. Taxonomic
54 information at the class and genus level are provided. Histograms show the relative
55 abundances (as counts per million, CPM) of *hsOTUs* at three sites. Dot plots show the
56 correlations between relative abundances of *hsOTUs* and phosphatase activities (only
57 significant positive correlation are shown, $P < 0.05$). Point size indicates the correlation
58 coefficient.

59 **Fig. S9** Co-occurrence networks visualizing the significant pairwise correlations ($r >$
60 0.8 , $P < 0.01$) between OTU pairs for bacteria in the hyphosphere, bacteria in the bulk
61 soil and AM fungi. The color of nodes indicates the associations of OTUs with different
62 experimental sites. The number of nodes, number of edges, average degree, and
63 *ssOTUs* are given below the specific networks.

64 **Fig. S10** The 16S rRNA gene copy number of the hyphosphere bacteria across three sites.

65 **Fig. S11** Mycorrhizal colonization (**a**) of host plants and hyphal length density (**b**) in
66 the hyphal compartments under each soil type in Experiment 2. Values are means ($n =$
67 8) and bars represent standard errors. Different letters indicate significant differences
68 among four soil types under the same inoculation treatment ($P < 0.05$).

69 **Fig. S12** Difference of P contents and phosphatase activities in the hyphal compartment
70 (HCs) inoculated or not inoculated with AM fungi in Experiment 2. (a) inorganic P, (b)
71 organic P, (c) alkaline phosphatase (ALP) activity and (d) acid phosphatase (ACP)
72 activity in the HCs. Data are means (n = 6) + standard error. HN indicates acidic red
73 soil collected from Hunan site, SX indicates loessial soil collected from Shaanxi site,
74 XJ indicates grey desert soil collected from Xinjiang site, and DB indicates black soil
75 collected from Jilin site. Different letters indicate significant differences among four
76 soil types ($P < 0.05$). The asterisk indicates significant differences between the hyphal
77 compartments with and without the presence of AM fungi. * $P < 0.05$, ** $P < 0.01$, ***
78 $P < 0.001$.

79 **Fig. S13** Profiling of hyphosphere bacterial communities in Experiment 2. a Histogram
80 diagram showing the relative abundances of major orders of hyphosphere and bulk soil
81 bacteria across four soil types. b Box plot showing Shannon-Wiener diversity indices
82 for bulk soil and hyphosphere bacterial communities. The asterisk indicates significant
83 difference between the bulk soil and the hyphosphere. c VENN plot showing the
84 number of OTUs enriched in the hyphosphere at each soil type. * $P < 0.05$, ** $P < 0.01$,
85 *** $P < 0.001$.

86 **Fig. S14** Qualitative taxonomic composition of module 4 (M4) in Experiment 1 and
87 module 30 (M30) in Experiment 2 is reported as proportional OTUs numbers per class.

88 **Table S1** Physicochemical properties of the soil used in Experiment 1 and 2.

89 **Table S2** The comparison between the hyphosphere core microbiome in our study and
90 the root-associated core microbiome in previous studies. “Y” represents “yes” under
91 “Also core in”. Further details of the maize and cotton root-associated core microbiome
92 can be found in Walters *et al.* (2018) and Zhang *et al.* (2022).

93 **Methods S1** Details of the experimental set-up.

94 **Experiment 1: field sampling experiment**

95 The field sampling experiment was carried out in three long-term soil fertility
96 experiments at Qiyang, Hunan Province; Yangling, Shaanxi Province; and Wulumuqi,
97 Xinjiang Province, China, representing moist, semiarid, and desert climatic conditions.
98 These three experimental sites belonged to The National Long-term Monitoring
99 Network of Soil Fertility and Fertilizer Effects, which was founded in 1990. To
100 characterize the complex interactions between AM fungi and hyphosphere bacteria *in*
101 *situ*, we buried in-growth tubes to collect AM fungal hyphae *in situ*. For each site, all
102 growth tubes were buried at the beginning of sowing and excavated at crop maturity in
103 2018, i.e. 90 days after being buried. Further details regarding soil properties, crop
104 rotation and climate conditions can be found in Zhang *et al.* (2009), Khan *et al.* (2018),
105 and Peng *et al.* (2021).

106 The complex problem of studying AM fungal-bacterial interactions under field
107 conditions was exemplified by how to retrieve the AM fungal hyphae from the soil. A
108 mixture of soil (< 30 μm) and glass beads has been used previously to collect hyphae
109 (Chen *et al.*, 2001; Zhang *et al.*, 2018). But this approach will change soil
110 physicochemical properties, and cannot explore the effects of soil types. Therefore, we
111 established two types of in-growth tubes (sealed with 30 or 0.45 μm mesh) combined
112 with the membrane to collect hyphae for this experiment (Fig. S1c, d). The membranes
113 with the above size of pores are usually used to study nutrient (e.g., N and P)
114 mobilization and utilization by the interaction between AM fungi and soil bacteria
115 (Hodge *et al.*, 2001; Zhang *et al.*, 2018).

116 The soil filling in the tubes was collected from the top 20 cm in the experimental
117 sites. In order to minimize the disturbance to the soil, we did not sterilize it. The soil
118 was passed through 2 mm sieve to remove root fragments, and then packed into tubes.
119 The soil bulk density varied from 1.2 to 1.5 $\text{g}^{-1} \text{cm}^3$ across three sites, and we took the
120 mean (1.35 $\text{g}^{-1} \text{cm}^3$). To make the results at the three sites comparable, we choose the
121 Loessial soil (SX site) as the benchmark, the weight of the soil that needs to be added
122 to the tubes is calculated based on the soil bulk density. The weight of the soil in the
123 tubes at the other two sites (HN and XJ) remained the same as for the SX site.

124 We imbedded the membranes in each tube to induce the growth of the hyphae on the
125 membrane (Fig. S1c). The membranes were sterilized by gamma irradiation (25 kGy,
126 ^{60}Co gamma rays). The principle is that the AM fungal hyphae enter the tube, and after

127 encountering the membrane, the hyphae grow and accumulate against the membrane,
128 which is convenient for collection. Firstly, we sealed one end of the tube with 30 or
129 0.45 μm mesh, then added one sixth amount (150 g) of the soil in the tube, gently
130 pressed the soil with a rod, and made the soil surface flat and centered. Then we put the
131 sterilized Poly tetra fluoro ethylene membrane (10 cm in diameter, Shanghaixinya
132 corporation, China) in the tube, and again added 150 g of the soil. We repeated the
133 above procedures until all five membranes were placed into the tube. Finally, we
134 pressed the soil and made the surface flat, and covered it with a 30 or 0.45 μm mesh
135 (Fig. S1c). In the tubes, the membranes were all tightly attached to the soil. The in-
136 growth tubes were buried in close proximity to the roots in the field (a depth of either
137 20-30 cm in soil 15 cm away from a plant; Fig. S1b). And the 30 μm mesh outside the
138 tubes did not hinder the growth of the hyphae into the tubes. The length of the in-growth
139 tube was only 5 cm, previous research has shown that AM fungal hyphae could grow
140 up to 12 cm from the root surface (Li *et al.*, 1991a). Therefore, the extraradical hyphae
141 of AM fungi colonizing the roots can successfully grow into the tubes and reach the
142 membrane surface. Moreover, the effects of the different pore sizes in the membranes
143 on bacterial migration and P diffusion can be neglected in this in-growth tube and has
144 been demonstrated to be negligible, so the bacteria can also access the tube freely (Li
145 *et al.*, 1991b; Zhang *et al.*, 2018; Zhang *et al.*, 2020).

146 We used a stereoscope to manually collect the hyphae accumulated on the surface of
147 membranes and measured the ratio of AM fungal and all fungal gene copy number to
148 validate that the vast majority of hyphae we chose were AM fungal hyphae (Fig. S2a).
149 The 0.45 μm membrane prevented AM fungal hyphae penetration, but allowed soil
150 solution flow and bacterial migration (Li *et al.*, 1991b; Zhang *et al.*, 2018; Zhang *et al.*,
151 2020). Importantly, hyphal exudates can act on the soil bacteria through the membrane.
152 As the mesh was tightly combined with soil before AM fungal mycelium arrived, the
153 hyphae on the mesh had a close contact with the fine soil particles (Fig. S1c, d).
154 Therefore, the bacteria on the surface of membrane living hyphae were consistent with
155 the microbiome on the soil living hyphae. And the mycelium segments collected from
156 the membrane can represent the mycelium growing in soil.

157

158 **Experimental 2: the microcosm experiment**

159 **Soil**

160 Soil was collected from locations within each of the same fields used in Experiment

161 1, plus a black soil collected from Changchun, Jilin. The collected soil was air dried,
162 sieved (2 mm) and the following nutrients were added to one kg of soil: 200 mg N
163 (NH_4NO_3), 200 mg K (K_2SO_4), 50 mg Mg ($\text{MgSO}_4 \cdot 7\text{H}_2\text{O}$), 5 mg Zn ($\text{ZnSO}_4 \cdot 7\text{H}_2\text{O}$), 5
164 mg Mn ($\text{MnSO}_4 \cdot \text{H}_2\text{O}$), and 2 mg Cu ($\text{CuSO}_4 \cdot 5\text{H}_2\text{O}$). The soil was sterilized by gamma
165 irradiation (25 kGy, ^{60}Co gamma rays) at the Beijing Atomic Energy Research Institute
166 to eliminate indigenous microorganisms and mycorrhizal propagules before use.

167 Microcosms

168 We used a compartmented microcosm system that separated the growing spaces of
169 root systems and the extraradical mycelium of AM fungi (Fig. S1e). The microcosms
170 were constructed using polyvinyl chloride (PVC) plates and consisted of root
171 compartments and hyphal compartments. The air buffer zone consisted of the PVC plate
172 with the 30 μm mesh glued on both sides (Fig. S1e), which allowed AM fungal hyphae
173 to pass through but prevented root penetration.

174 Host plants

175 Maize (*Zea mays* L., cv. Zhengdan 958) was used as the host plant. The seeds were
176 surface-sterilized with 10% (v/v) H_2O_2 for 10 min and 70% (v/v) ethanol for 3 min and
177 then rinsed eight times with sterile deionized water. After imbibing water at 27°C in the
178 dark for 2 d, the seedlings were sown into the microcosms.

179 AM fungal and bacterial inoculant

180 The AM fungal strain *Rhizophagus intraradices* EY108 was selected as inoculant,
181 and was purchased from the International Collection of (Vesicular) Arbuscular
182 Mycorrhizal Fungi (West Virginia University, Morgantown, WV). The inocula was
183 propagated for 8 months in a mixture of zeolite and river sand (5:1, w:w) using maize
184 and plantago as the host plants in the greenhouse. The inocula consisted of substrate
185 containing spores (approximate 8 spores g^{-1} substrate), mycelium and fine root
186 segments. The filtrate of each soil type was obtained by suspending 30 g of each soil in
187 300 mL of sterile water and filtration through six-layer quantitative filter paper,
188 respectively. This allowed the passage of common soil microbes but effectively retained
189 AM fungal spores and hyphae. A total of 10 mL of each soil filtrate was added to the
190 hyphal compartments as the original microflora.

191 Experimental design and procedure

192 The microcosm experiment contained the following treatments: four soil types,
193 including acidic red soil, loessial soil, grey desert soil and black soil, and with or
194 without AM fungal inocula. Each treatment had six replicates, which were arranged in

195 a randomized block design in a glasshouse. At planting, 600 g soil for each root
196 compartment was carefully added to the root compartment, and then 60 g AM fungal
197 inoculum was added to each root compartment. Finally, three pre-germinated seeds
198 were sown, and the remaining 250 g soil was added to the root compartments. 900 g
199 soil for each hyphal compartment was added. The control treatments (NM) received the
200 same amount of sterilized inoculum. Seven days after sowing, the seedlings were
201 thinned to one in each microcosm. During the experiment, soil moisture was kept at 18-
202 20% (w/w, c. 70% of field moisture capacity) as determined gravimetrically by
203 weighing the pots every 2 days and adding water as necessary. Plants in these
204 microcosms were grown in the glasshouse at China Agricultural University in Beijing
205 from 1 May to 9 July 2019.

206 **DNA extraction and PCR**

207 To identify the AM fungal taxa in Experiment 1, an approximately 334 bp region of
208 18S rRNA gene was amplified with a two-step PCR (Yang *et al.*, 2018). In the first
209 round, GeoA-2 (5'-CCAGTAGTCATATGCTTGTCTC-3') and AML2 (5'-
210 GAACCCAAACACTTTGGTTTCC-3') primer pairs were used (Schwarzott &
211 Schussler, 2001; Lee *et al.*, 2008). The PCR amplification was carried out in a total
212 volume of 25 μ L, including 12.5 μ L 2 \times Taq Plus Master Mix, 3 μ L BSA, 6.5 μ L ddH₂O,
213 1 μ L of each primer (5 μ M), and 1 μ L template DNA. The thermal cycling was followed
214 by an initial denaturation at 94°C for 2 min, 35 cycles of denaturation at 94°C for 30 s,
215 annealing at 59°C for 1 min, and extension at 72°C for 2 min, followed by a final
216 extension at 72°C for 7 min. The products of the first amplification were diluted for 10
217 times with sterilized deionized water and 1.0 μ L diluted solution was used as the
218 template for the nested PCR. The second round of PCR was performed with AMDGR
219 (5'-TTGGAGGGCAAGTCTGGTGCC-3') and NS31 (5'-
220 CCCAACTATCCCTATTAATCAT-3') primer pairs (Simon *et al.*, 1992; Helgason *et al.*,
221 1998). Both forward and reverse primers were augmented with 8 bp long barcodes
222 unique to each sample. The conditions of the nested PCR were similar to the first PCR,
223 except for 35 cycles of denaturation at 94°C for 30 s, annealing at 58°C for 1 min, and
224 extension at 72°C for 1 min.

225 To identify the bacterial taxa in both experiments, the V3-V4 regions of the bacterial
226 16S rRNA gene were amplified with primer pairs 338F (5'-
227 ACTCCTACGGGAGGCAGCAG-3') and 806R (5'-
228 GGACTACHVGGGTWTCTAAT-3') (Sakurai *et al.*, 2008). Both forward and reverse

229 primers were augmented with 5-8 bp long barcodes unique to each sample. The PCR
230 amplification was performed in a total volume of 25 μ L, containing 12.5 μ L 2 \times Taq Plus
231 Master Mix, 1 μ L of each primer (5 μ M), 1 μ L DNA template, 3 μ L BSA and 6.5 μ L
232 ddH₂O. The PCR program consisted of an initial denaturation at 94°C for 5 min; 28
233 cycles of 30 s of denaturation at 94°C, 30 s of annealing at 55°C and 60 s of elongation
234 at 72°C; and 7 min of final elongation at 72°C.

235 **Bioinformatic processing**

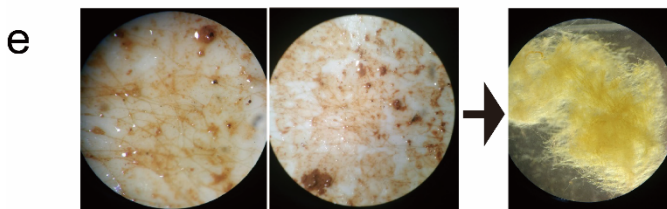
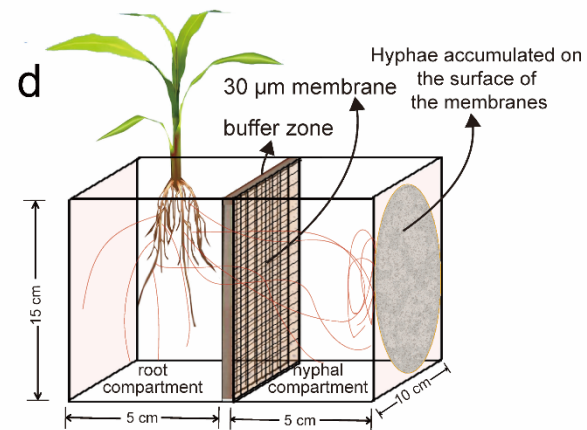
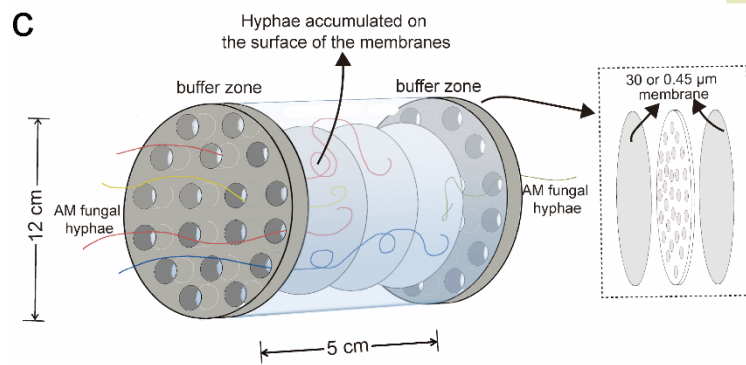
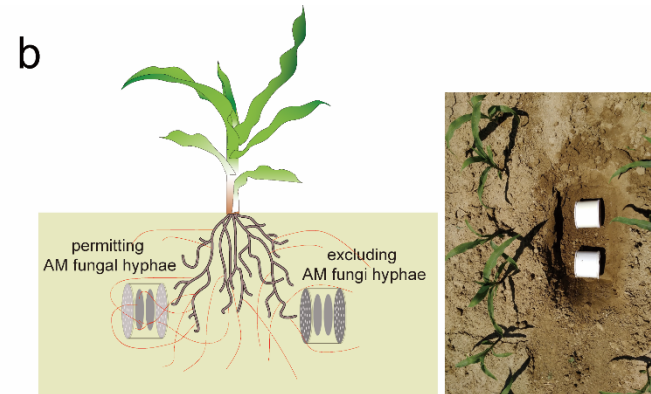
236 The raw data were first screened, and sequences were removed from consideration if
237 they were shorter than 230 bp, had a low-quality score (≤ 20), contained ambiguous
238 bases or did not exactly match to primer sequences and barcode tags, and separated
239 using the sample-specific barcode sequences. Qualified reads were clustered into
240 operational taxonomic units (OTUs) at a similarity level of 97% use Uparse algorithm
241 of Vsearch (v2.7.1) software (Edgar, 2013). The Ribosomal Database Project (RDP)
242 Classifier tool was used to classify all sequences into different taxonomic groups
243 against SILVA132 database (Quast *et al.*, 2013). QIIME (v1.8.0) was used to calculate
244 the richness and diversity indices based on the OTU information.

245 **Real time q-PCR analysis of 16S rRNA, AM fungal and total fungal gene**

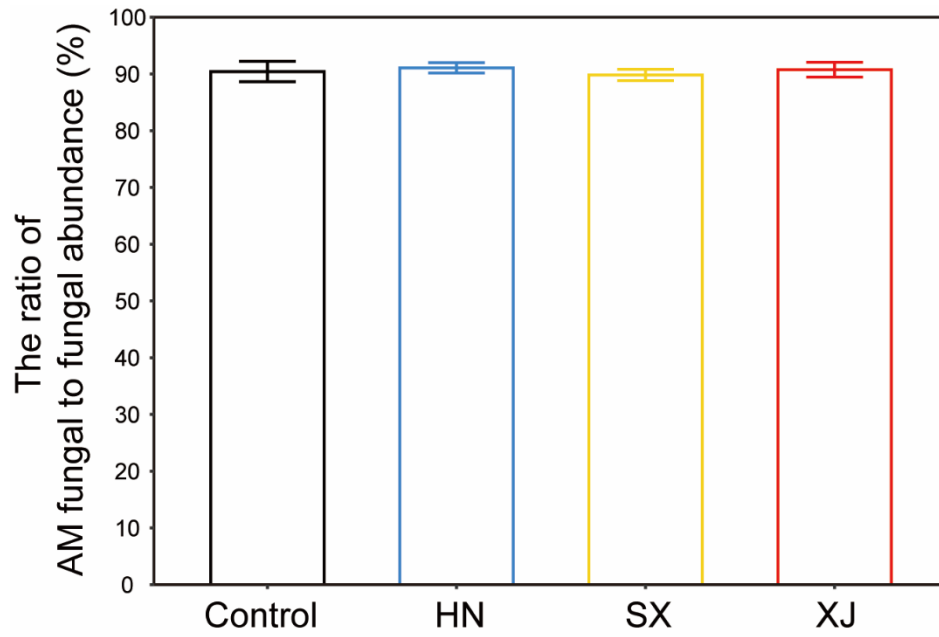
246 To determine the copy numbers of hyphosphere bacteria, AM fungi and total fungi
247 in our hyphal samples, the DNA extracted from hyphal samples was quantified in
248 triplicate by real-time q-PCR using q-PCR analyzer TIB8600 (Triplex Bioscience
249 (China) Co., Ltd., Xiamen, China) with 16S rRNA, AM fungal and total fungal gene
250 specific primers. The primer sets were 515F (5'-GTGCCAGCMGCCGCGGTAA-
251 3')/907R (5'-CCGTCAATTCMTTTRAGTTT-3'), AMV4.5NF (5'-
252 CGCCCGCCGCGCGGGCGGGCGGGGCGGGGGCACGGGGGG [GC clamp]
253 AAGCTCGTAGTTGAATTTTCG-3')/AMDGR (5'-CCCAACTATCCCTATTAATCAT-
254 3') and 5.8s (CGCTGCGTTCTTCATCG)/ITS1f (TCCGTAGGTGAACCTGCGG)
255 targeting for bacteria, AM fungi and all fungi, respectively (Sato *et al.*, 2005; Sakurai
256 *et al.*, 2008; Rousk *et al.*, 2010). SYBR Green real time q-PCR Master Mix (TOYOBO,
257 Japan) was used and conducted under the following reaction conditions: initial
258 denaturation at 95°C for 5 min; 40 cycles consisting of denaturation at 95°C for 15 s,
259 annealing at 60°C for 30 s, and elongation at 72°C for 1 min. Fluorescence of SYBR
260 green was detected after every cycle. The dissolution curve was collected when the
261 whole reaction ended in 0.5°C increments from 65°C to 95°C. No amplification was
262 detected in the negative controls. The plasmid was sequenced for verification before

263 constructing a standard curve for absolute quantification of gene copy. The standard
264 curve was prepared in triplicate using five serial 10-fold dilutions, and quantification
265 calculated by determining the starting copy number by considering the concentration
266 of the plasmid and number of base pairs (vector plus primer).

267 **Fig. S1** Details of the experimental sites and experimental system. **a** Geographical location of the three experimental sites in China. **b** The in-
268 growth tubes were buried to a depth of 20-30 cm in soil and 15 cm away from the plants. PVC tubes (12 cm in diameter, 5 cm in length) were
269 sealed with 30 μm mesh (permitting AM fungal hyphae but not roots to grow into) or 0.45 μm membrane (excluding AM fungal hyphae and roots
270 to grow into) in the two ends, respectively. **c** Schematic drawing of the in-growth tubes. **d** Schematic drawing of the two-compartment cultivation
271 system (microcosm) used in the pot experiment. The microcosm is divided into a root compartment and a hyphal compartment by two 30 μm nylon meshes and
272 a buffer zone. **e** The hyphae accumulated on the surface of the membranes. AM fungal hyphae were manually collected using a stereoscope,
273 according to their different characteristics from other fungi. AM fungal hyphae are colorless and transparent, and have no septum. The collected
274 hyphae were washed five times in washing buffers (0.01 M Phosphate buffer saline, pH = 7) to remove the adhered soil.

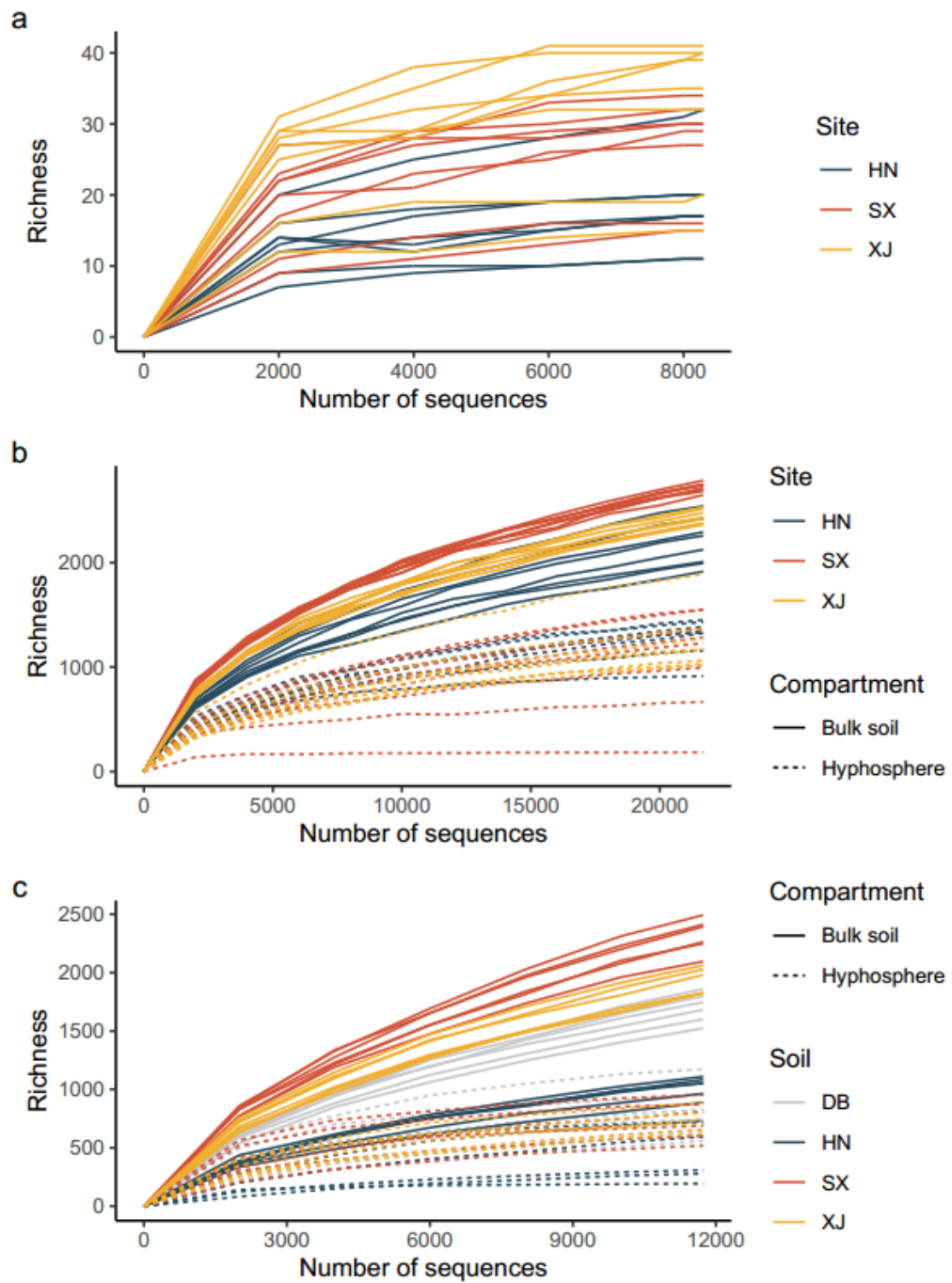


276 **Fig. S2** The ratio of AM fungal to total fungal DNA copy number in hyphal samples across
277 three sites. The higher the ratio, the greater the proportion of AM fungi in our hyphal samples.
278 Control indicates the pure AM fungal hyphal samples collected from AM fungal inoculum.
279 Values are means (n = 8) and bars represent standard errors.

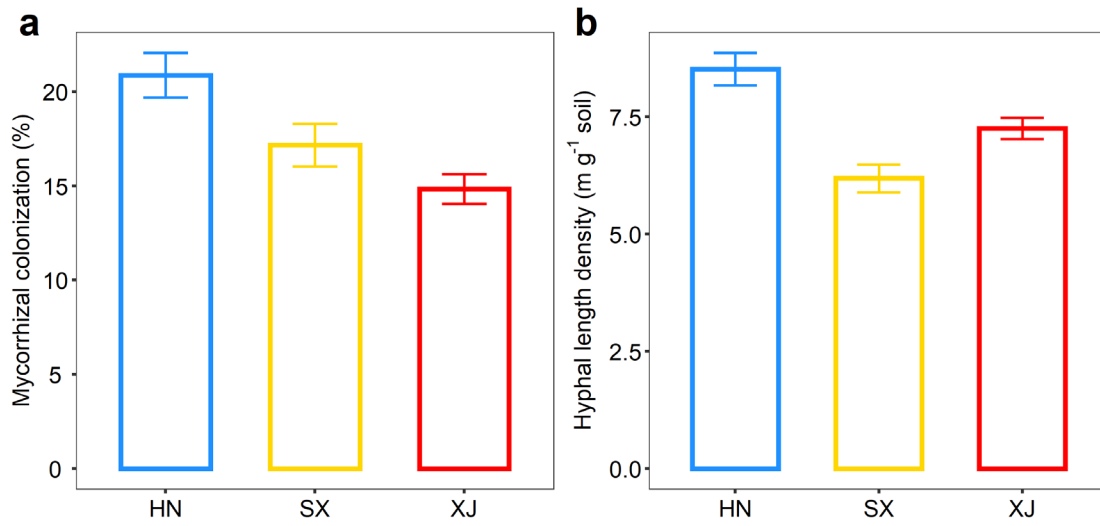


280 **Fig. S3** Rarefaction curve of OTUs for individual sample across the different datasets:
 281 (a) AM fungal 18S rRNA gene dataset in Experiment 1, (b) hyphosphere and bulk soil
 282 bacterial 16S rRNA gene dataset in Experiment 1, c hyphosphere and bulk soil bacterial
 283 16S rRNA gene dataset in Experiment 2.

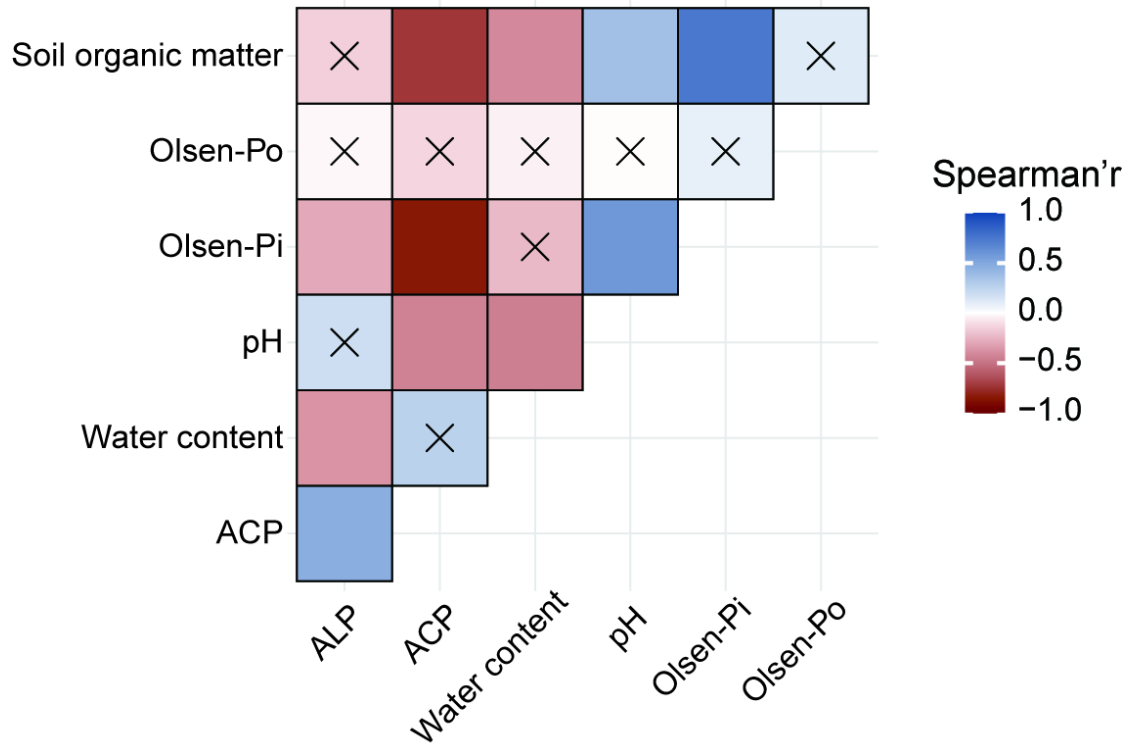
284



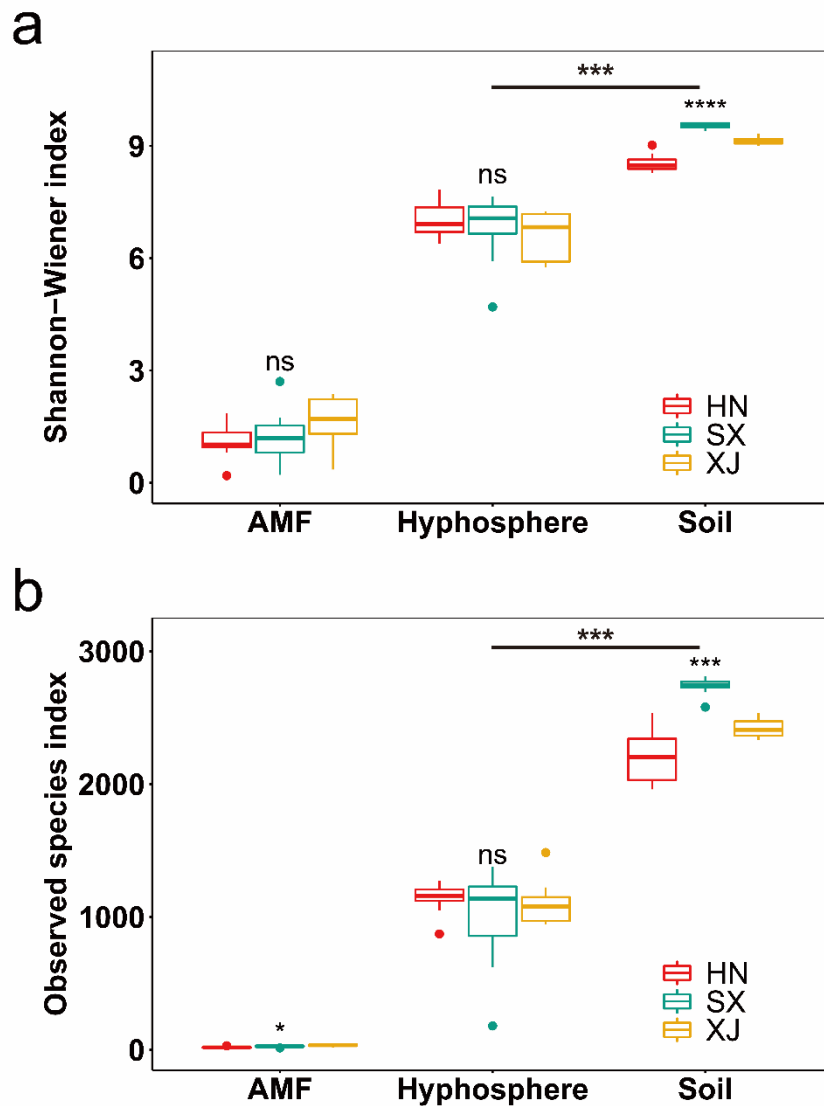
285 **Fig. S4** Mycorrhizal colonization (**a**) of host plants and hyphal length density (**b**) in the
286 in-growth tubes at each site. Values are means (n = 8) and bars represent standard errors.



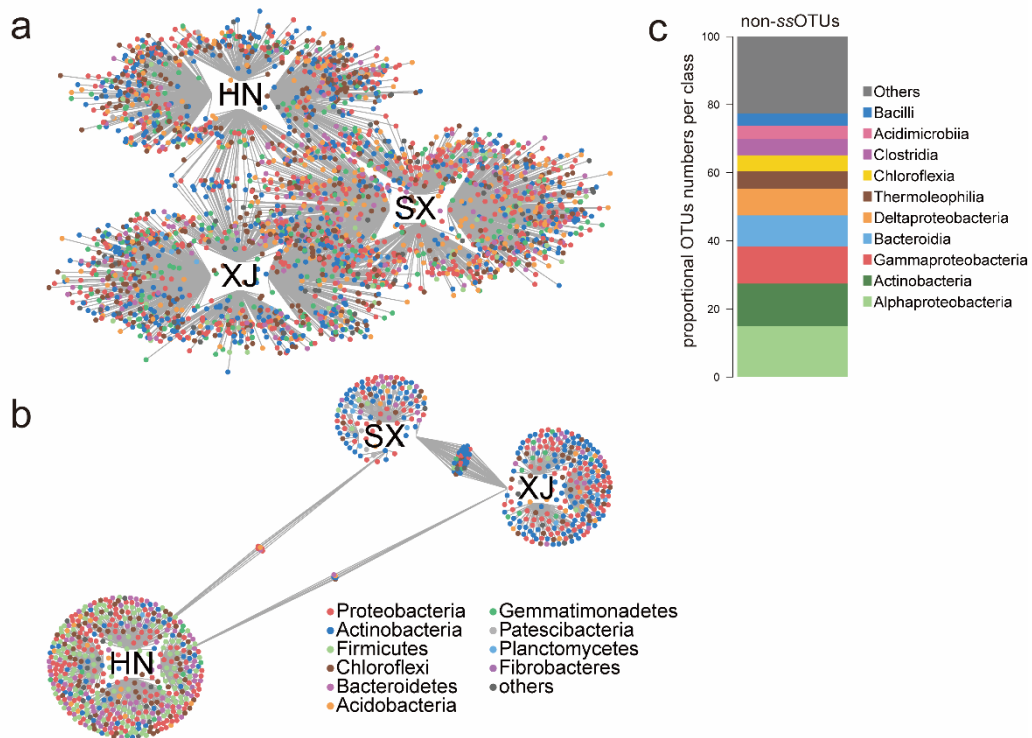
287 **Fig. S5** Correlation matrix (Spearman) of phosphatase activities and soil properties in
 288 the tubes across the three sites. Positive correlations are displayed in red and negative
 289 correlations in blue. Color intensity is proportional to the correlation coefficients.
 290 Correlations significant at $P < 0.05$ were not marked with a cross.



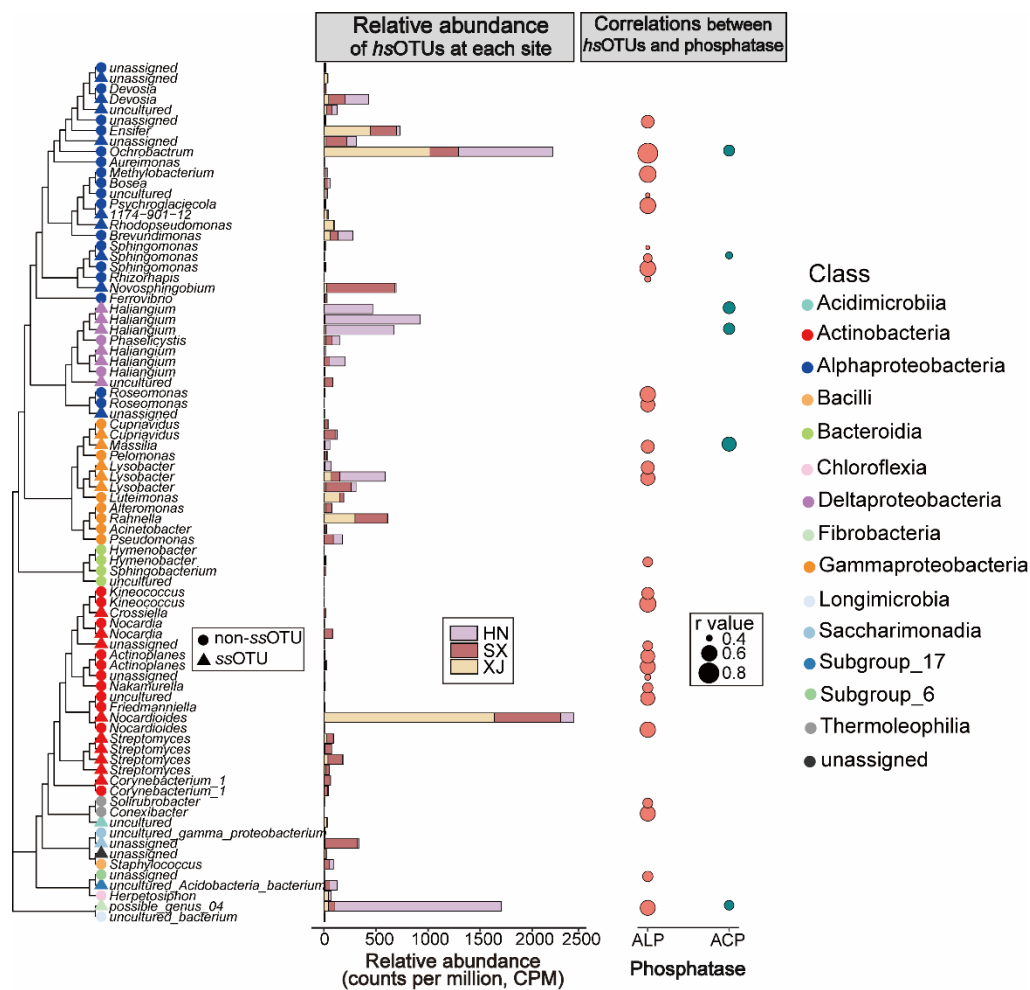
291 **Fig. S6** Box plot showing Shannon-Wiener diversity indices (a) and observed species indices (b) for three communities (AM fungi, hyphosphere and bulk soil bacteria). For
 292 each community, the asterisk indicates significant difference among three sites. The
 293 asterisk on the solid line represented the significant difference between bacteria in the
 294 hyphosphere and bulk soil. Boxes show first quartile, median and third quartile.
 295 Whiskers extend to the most extreme points within $1.5 \times$ box length, and the points are
 296 values that fall outside the whiskers. * $P < 0.05$, ** $P < 0.01$, *** $P < 0.001$, **** $P <$
 297 0.0001 . ns, no significance.



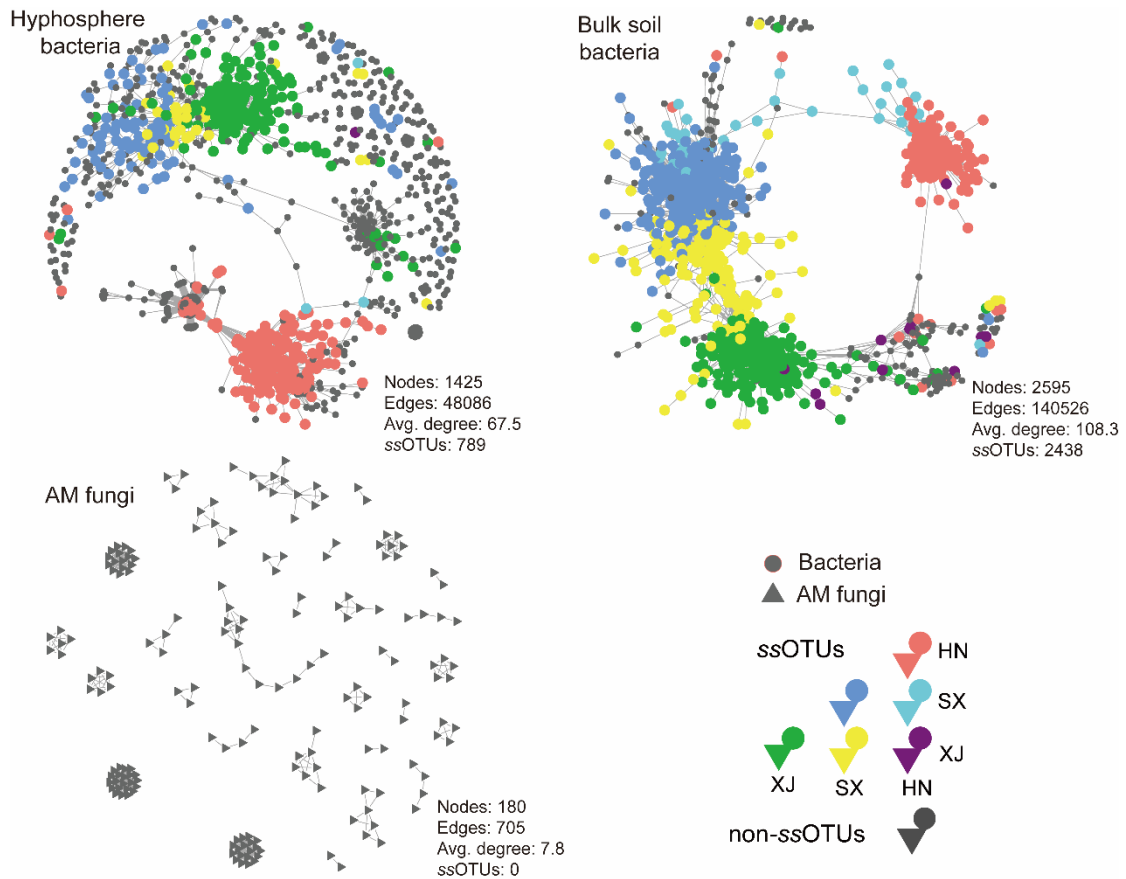
299 **Fig. S7** Bipartite networks display experimental site-sensitive OTUs (*ssOTUs*) in bulk
 300 soil **(a)** and hyphosphere **(b)** bacterial communities. Circles represented individual
 301 bacterial OTUs that are positively and significantly associated ($P < 0.05$) with one or
 302 more of sites (associations given by connecting lines). OTUs were colored according
 303 to their phyla assignment. **c** Qualitative taxonomic composition of experimental site-
 304 insensitive OTUs (*non-ssOTUs*) is reported as proportional OTUs numbers per class.
 305



306 **Fig. S8** *hsOTUs* are largely conserved at the class levels across three experimental sites.
 307 Phylogenetic characterization was conducted using a neighbor-joining model of 82
 308 *hsOTUs*. Circles represent non-*ssOTUs* and triangles represent *ssOTUs*. Taxonomic
 309 information at the class and genus level are provided. Histograms show the relative
 310 abundances (as counts per million, CPM) of *hsOTUs* at three sites. Dot plots show the
 311 correlations between relative abundances of *hsOTUs* and phosphatase activities (only
 312 significant positive correlation are shown, $P < 0.05$). Point size indicates the correlation
 313 coefficient.

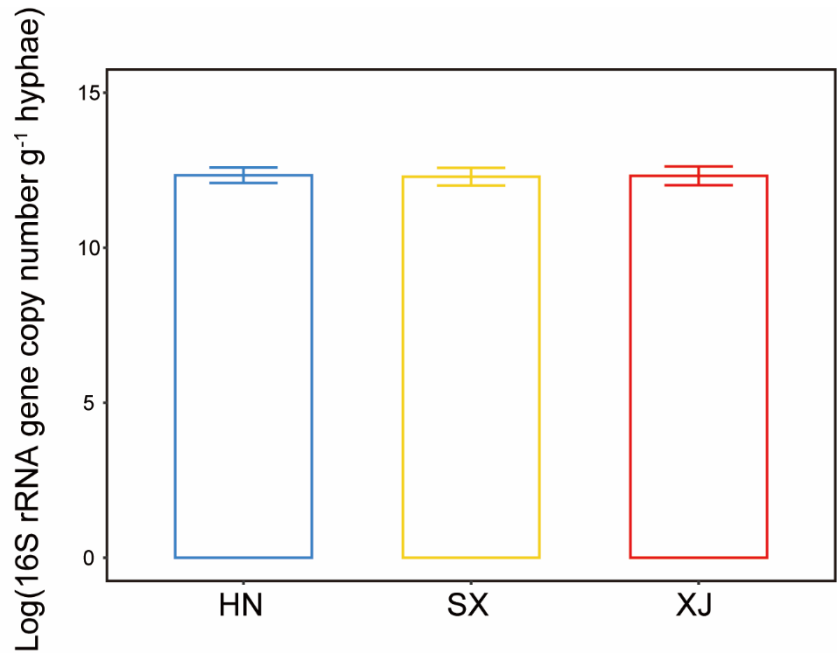


314 **Fig. S9** Co-occurrence networks visualizing the significant pairwise correlations ($r >$
 315 0.8 , $P < 0.01$) between OTU pairs for bacteria in the hyphosphere, bacteria in the bulk
 316 soil and AM fungi. The color of nodes indicates the associations of OTUs with different
 317 experimental sites. The number of nodes, number of edges, average degree, and
 318 ssOTUs are given below the specific networks.

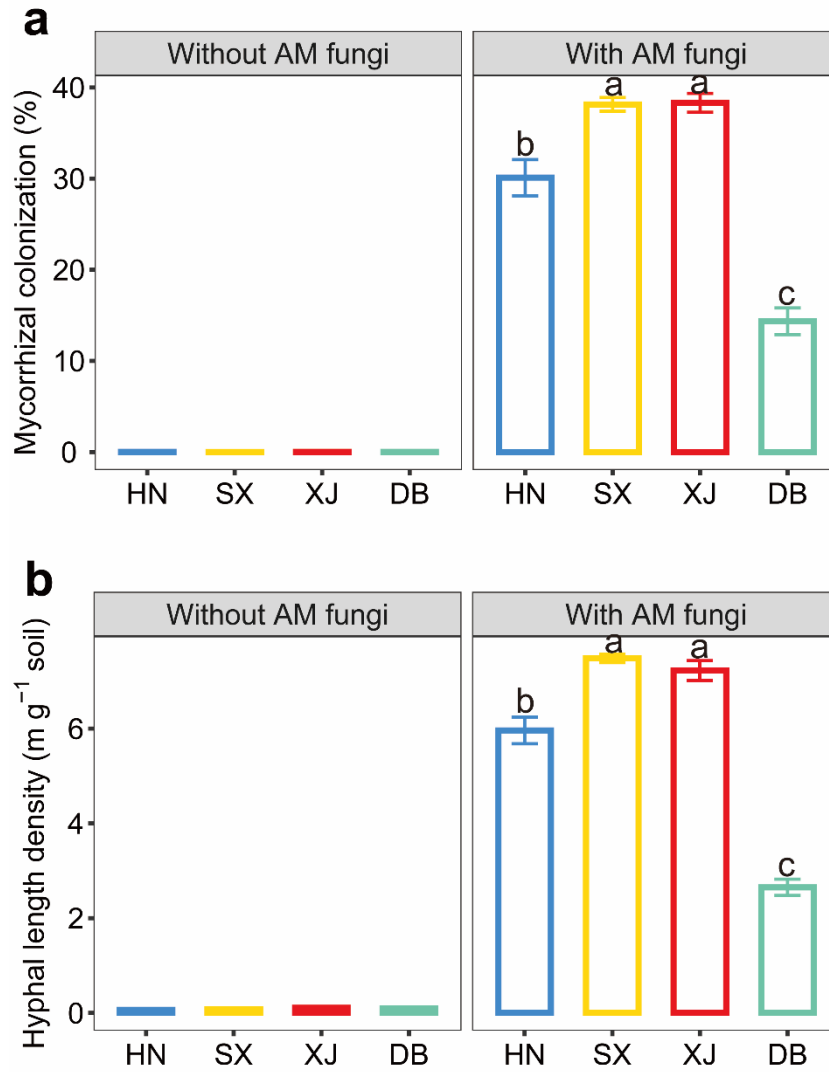


319 **Fig. S10** The 16S rRNA gene copy number of the hyphosphere bacteria across three sites.

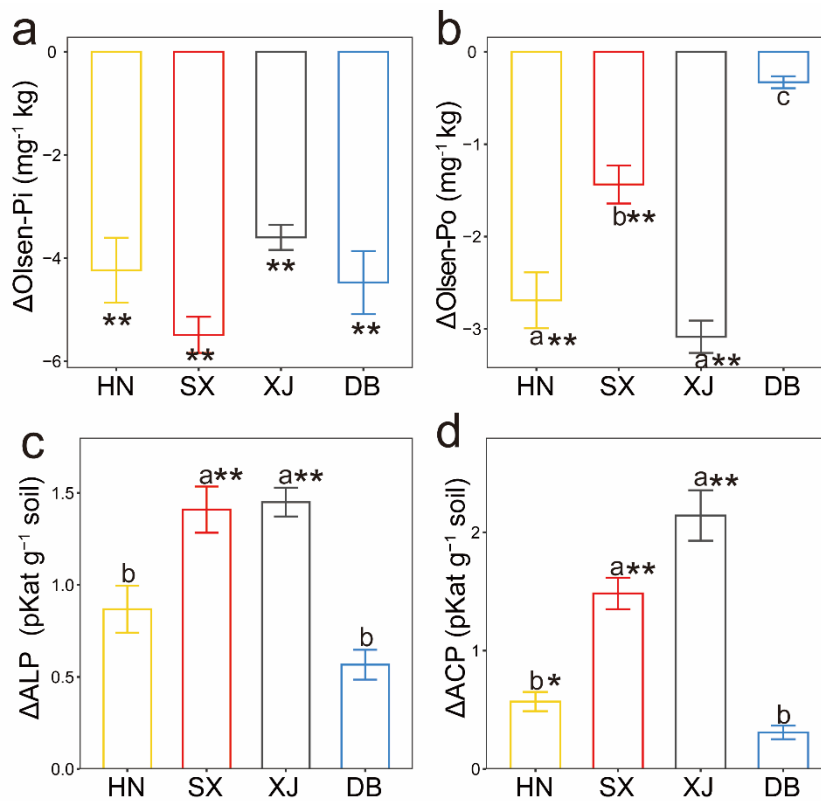
320 Values are means (n = 8) and bars represent standard errors.



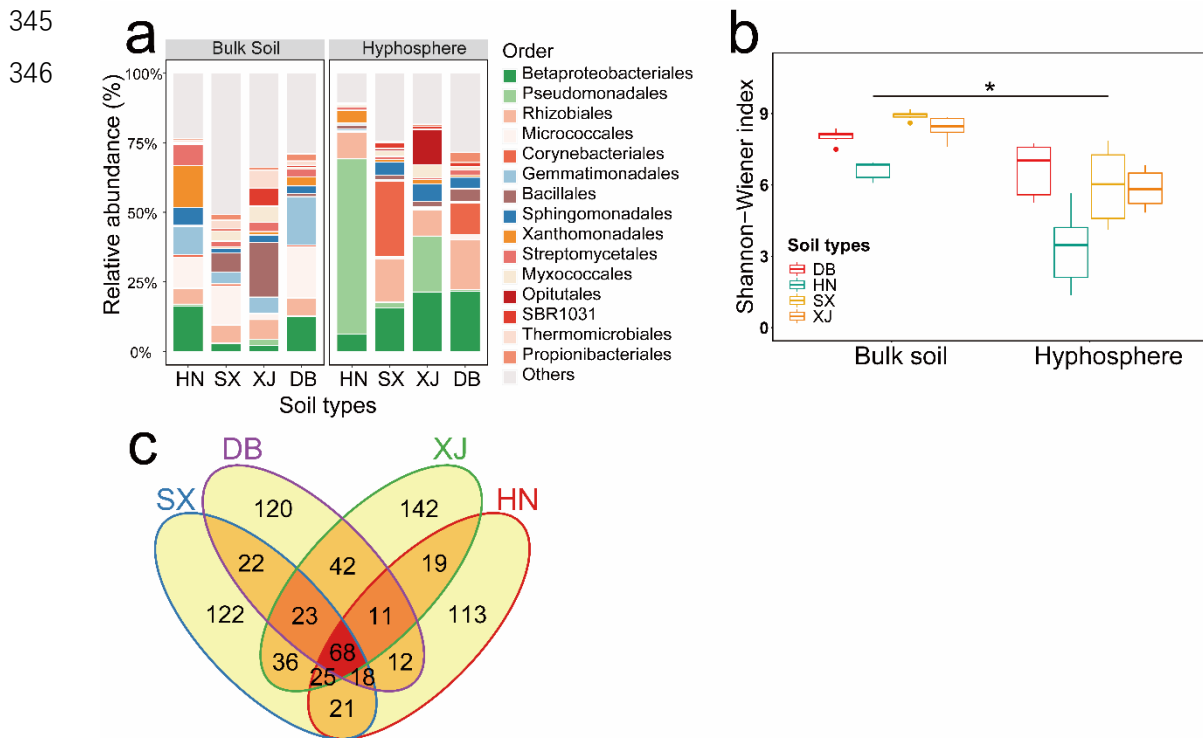
321 **Fig. S11** Mycorrhizal colonization (**a**) of host plants and hyphal length density (**b**) in
322 the hyphal compartments under each soil type in Experiment 2. Values are means (n =
323 8) and bars represent standard errors. Different letters indicate significant differences
324 among four soil types under the same inoculation treatment ($P < 0.05$).
325



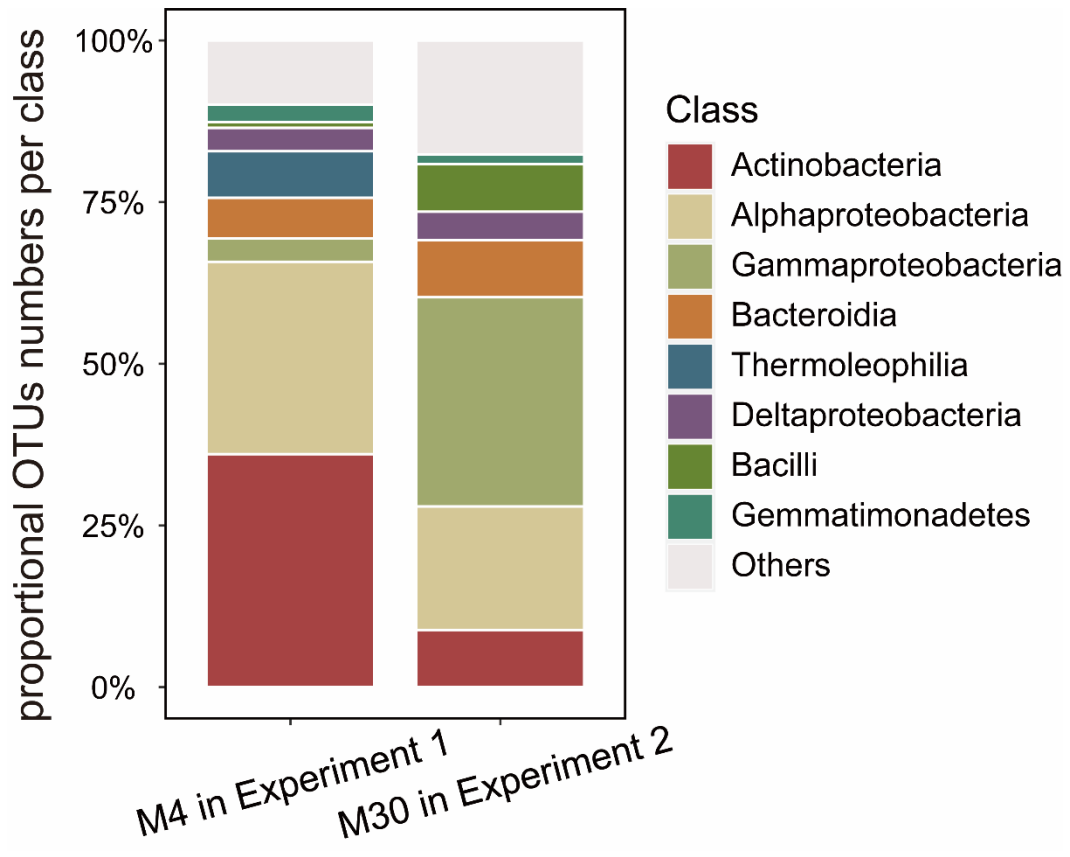
326 **Fig. S12** Difference of P contents and phosphatase activities in the hyphal compartment
 327 (HCs) inoculated or not inoculated with AM fungi in Experiment 2. **(a)** inorganic P, **(b)**
 328 organic P, **(c)** alkaline phosphatase (ALP) activity and **(d)** acid phosphatase (ACP)
 329 activity in the HCs. Data are means (n = 6) + standard error. HN indicates acidic red
 330 soil collected from Hunan site, SX indicates loessial soil collected from Shaanxi site,
 331 XJ indicates grey desert soil collected from Xinjiang site, and DB indicates black soil
 332 collected from Jilin site. Different letters indicate significant differences among four
 333 soil types ($P < 0.05$). The asterisk indicates significant differences between the hyphal
 334 compartments with and without the presence of AM fungi. * $P < 0.05$, ** $P < 0.01$, ***
 335 $P < 0.001$. ns, no significance.



336 **Fig. S13** Profiling of hyphosphere bacterial communities in Experiment 2. **a** Histogram
 337 diagram showing the relative abundances of major orders of hyphosphere and bulk soil
 338 bacteria across four soil types. **b** Box plot showing Shannon-Wiener diversity indices
 339 for bulk soil and hyphosphere bacterial communities. The asterisk indicates significant
 340 difference between the bulk soil and the hyphosphere. **c** VENN plot showing the
 341 number of OTUs enriched in the hyphosphere at each soil type. Boxes show first
 342 quartile, median and third quartile. Whiskers extend to the most extreme points within
 343 $1.5 \times$ box length, and the points are values that fall outside the whiskers. * $P < 0.05$, **
 344 $P < 0.01$, *** $P < 0.001$.



347 **Fig. S14** Qualitative taxonomic composition of module 4 (M4) in Experiment 1 and
348 module 30 (M30) in Experiment 2 is reported as proportional OTUs numbers per class.



349 **Table S1** Physicochemical properties of the soil used in Experiment 1 and 2.

	Soil types			
	Acidic red soil	Loessial soil	Grey desert soil	Black soil
Origination	Hunan Province (111°52' E, 26°45'N)	Shaanxi Province (108°00'E, 34°17'N)	Xinjiang Province (87°46'E, 43°57'N)	Jilin Province (43°54'E, 125°18' N)
Used in Experiment 1 or Experiment 2	Experiment 1 and 2	Experiment 1 and 2	Experiment 1 and 2	Experiment 2
Soil classification (FAO)	Haplic Calcisols	Calcaric Regosol	Ferralic Cambisol	Haplic Phaeozem
Olsen inorganic P (mg kg ⁻¹)	10.11	24.97	11.98	48.89
Olsen organic P (mg kg ⁻¹)	6.89	6.78	5.98	15.77
Soil pH	6.55	7.94	8.00	7.78
Soil organic matter (g kg ⁻¹)	5.51	11.12	7.68	18.72

350 **Table S2** The comparison between the hyphosphere core microbiome in our study and the root-associated core microbiome in previous studies.
 351 “Y” represents “yes” under “Also core in”. Further details of the maize and cotton root-associated core microbiome can be found in Walters *et al.*
 352 (2018) and Zhang *et al.* (2022).

Taxonomy			Also core in:	
Phylum	Class	Order	maize	cotton
Actinobacteria	Actinobacteria	Corynebacteriales		
		Frankiales		
		Pseudonocardiales	Y	Y
Proteobacteria	Alphaproteobacteria	Rhizobiales	Y	Y
Firmicutes	Bacilli	Bacillales		Y
Bacteroidetes	Bacteroidia	Chitinophagales		
		Cytophagales		
Chloroflexi	Chloroflexia	Chloroflexales		
Proteobacteria	Deltaproteobacteria	Myxococcales		
		Alteromonadales		
	Gammaproteobacteria	Betaproteobacteriales	Y	Y
		Enterobacteriales		
		Xanthomonadales	Y	

353

354 **References**

- 355 **Chen BD, Christie P, Li XL. 2001.** A modified glass bead compartment cultivation
356 system for studies on nutrient and trace metal uptake by arbuscular mycorrhiza.
357 *Chemosphere* **42**(2): 185-192.
- 358 **Edgar RC. 2013.** UPARSE: highly accurate OTU sequences from microbial amplicon
359 reads. *Nature Methods* **10**(10): 996-+.
- 360 **Helgason T, Daniell TJ, Husband R, Fitter AH, Young JPW. 1998.** Ploughing up the
361 wood-wide web? *Nature* **394**(6692): 431-431.
- 362 **Hodge A, Campbell CD, Fitter AH. 2001.** An arbuscular mycorrhizal fungus
363 accelerates decomposition and acquires nitrogen directly from organic material.
364 *Nature* **413**: 297–299.
- 365 **Khan A, Lu GY, Ayaz M, Zhang HT, Wang RJ, Lv FL, Yang XY, Sun BH, Zhang
366 SL. 2018.** Phosphorus efficiency, soil phosphorus dynamics and critical
367 phosphorus level under long-term fertilization for single and double cropping
368 systems. *Agriculture Ecosystems & Environment* **256**: 1-11.
- 369 **Li XL, George E, Marschner H. 1991a.** Extension of the phosphorus depletion zone
370 in VA-mycorrhizal white clover in a calcareous soil. *Plant and Soil* **136**(1): 41-
371 48.
- 372 **Li XL, George E, Marschner H. 1991b.** Phosphorus depletion and pH decrease at the
373 root–soil and hyphae–soil interfaces of VA mycorrhizal white clover fertilized
374 with ammonium. *New Phytologist* **119**(3): 397-404.
- 375 **Lee J, Lee S, Young JPW. 2008.** Improved PCR primers for the detection and
376 identification of arbuscular mycorrhizal fungi. *Fems Microbiology Ecology*
377 **65**(2): 339-349.
- 378 **Peng Y, Duan YS, Huo WG, Xu MG, Yang XY, Wang XH, Wang BR, Blackwell
379 MSA, Feng G. 2021.** Soil microbial biomass phosphorus can serve as an index
380 to reflect soil phosphorus fertility. *Biology and Fertility of Soils* **57**(5): 657-669.
- 381 **Quast C, Pruesse E, Yilmaz P, Gerken J, Schweer T, Yarza P, Peplies J, Glockner
382 FO. 2013.** The SILVA ribosomal RNA gene database project: improved data
383 processing and web-based tools. *Nucleic Acids Research* **41**(Database issue):
384 D590-596.
- 385 **Rousk J, Baath E, Brookes PC, Lauber CL, Lozupone C, Caporaso JG, Knight R,
386 Fierer N. 2010.** Soil bacterial and fungal communities across a pH gradient in

387 an arable soil. *ISME Journal* **4**(10): 1340-1351.

388 **Sakurai M, Wasaki J, Tomizawa Y, Shinano T, Osaki M. 2008.** Analysis of bacterial
389 communities on alkaline phosphatase genes in soil supplied with organic matter.
390 *Soil Science and Plant Nutrition* **54**(1): 62-71.

391 **Sato K, Suyama Y, Saito M, Sugawara K. 2005.** A new primer for discrimination of
392 arbuscular mycorrhizal fungi with polymerase chain reaction-denature gradient
393 gel electrophoresis. *Grassland Science* **51**(2): 179-181.

394 **Schwarzott D, Schussler A. 2001.** A simple and reliable method for SSU rRNA gene
395 DNA extraction, amplification, and cloning from single AM fungal spores.
396 *Mycorrhiza* **10**(4): 203-207.

397 **Simon L, Lalonde M, Bruns TD. 1992.** Specific amplification of 18S fungal
398 ribosomal genes from vesicular-arbuscular endomycorrhizal fungi colonization
399 roots. *Applied and Environmental Microbiology* **58**(1): 291-295.

400 **Walters WA, Jin Z, Youngblut N, Wallace JG, Sutter J, Zhang W, Gonzalez-Pena**
401 **A, Peiffer J, Koren O, Shi Q, et al. 2018.** Large-scale replicated field study of
402 maize rhizosphere identifies heritable microbes. *Proceedings of the National*
403 *Academy of Sciences of the United States of America* **115**(28): 7368-7373.

404 **Yang W, Gu S, Xin Y, Bello A, Sun W, Xu X. 2018.** Compost addition enhanced
405 hyphal growth and sporulation of arbuscular mycorrhizal fungi without
406 affecting their community composition in the soil. *Frontiers in Microbiology* **9**.

407 **Zhang WJ, Xu MG, Wang BR, Wang XJ. 2009.** Soil organic carbon, total nitrogen
408 and grain yields under long-term fertilizations in the upland red soil of southern
409 China. *Nutrient Cycling in Agroecosystems* **84**(1): 59-69.

410 **Zhang K, Maltais-Landry G, George S, Grabau ZJ, Small IM, Wright D, Liao HL.**
411 **2022.** Long-term sod-based rotation promotes beneficial root microbiomes and
412 increases crop productivity. *Biology and Fertility of Soils* **58**(4): 403-419.

413 **Zhang L, Peng Y, Zhou J, George TS, Feng G. 2020.** Addition of fructose to the
414 maize hyphosphere increases phosphatase activity by changing bacterial
415 community structure. *Soil Biology and Biochemistry* **142**.

416 **Zhang L, Shi N, Fan J, Wang F, George TS, Feng G. 2018.** Arbuscular mycorrhizal
417 fungi stimulate organic phosphate mobilization associated with changing
418 bacterial community structure under field conditions. *Environmental*
419 *Microbiology* **20**(7): 2639-2651.